PI PLUS STATE OBSERVER CONTROL OF ELECTROMAGNETIC VIBRATORY FEEDER

Aleksandar I. Ribić, Željko V. Despotović, *Institut Mihajlo Pupin, Beograd,aleksandar.ribic@automatika.imp.bg.ac.yu*

Abstract – *In this paper, a high performance feedback controller for electromagnetic vibratory feeder is proposed. The controller structure consists of a PI controller combined with the state observer. The controlled variable is the resonant frequency vibration amplitude obtained in real time from the state observer. Use of the state observer allows fast disturbance rejection and reference tracking in both directions (amplitude increase and decrease). Simulations and experimental results from the real device are presented.*

1. INTRODUCTION

A VIBRATION FEEDER is widely used device for transport of granular and particulate material in various food manufacturing industries. Electromagnetic Vibratory Feeders (EVF) are a very popular because of their high efficiency and easy maintenance. However, their performance is highly sensitive to different kind of disturbances. For example, as the feeder vibrations occurred at its resonance frequency, vibration amplitude is highly dependent on a damping factor. On the other hand, damping factor depends on the mass of material on the feeder through, type of material, and the vibration amplitude [1]. These disturbances can reduce drastically (up to 10 times) the vibration amplitude, thus reducing the performance of EVF.

In the present paper by combining a feedback PI controller with a state observer, a fast set point and disturbance rejection responses of the EVF are obtained. Controller is implemented on industrial PC platform and applied to the experimental feeder. Simulations and experimental results confirm effectiveness of the proposed controller.

2. EVF DESCRIPTION

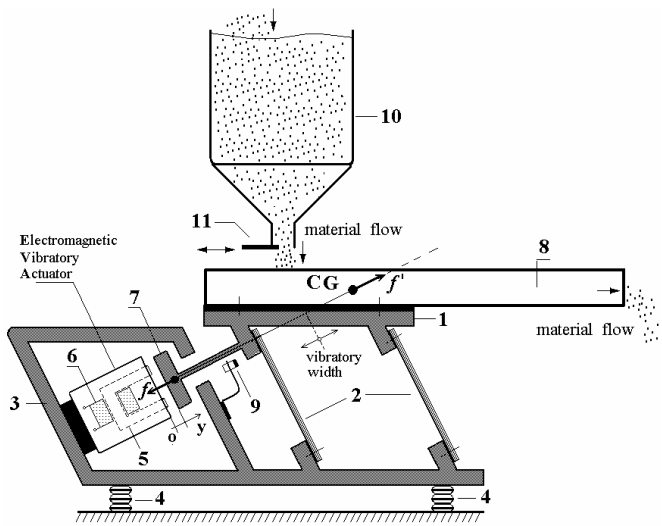

Fig.1. *Typical construction of vibratory feeder (conveyor) with electromagnetic drive*

A typical arrangement of EVF can be seen in Fig.1. Its main components are the load carry element (LCE) **1**, electromagnetic vibratory actuator (EVA) as source of excitation force f and flexible elements **2**.

Flexible elements **2** are made of composite leaf springs. These elements are rigidly connected to the base **3**, which is resting on rubber pads **4** to the foundation. Magnetic core **5** is covered by continuous windings coil **6**. Electromagnetic force f acts on armature **7** attached to the LCE. This element carries the vibratory trough **8** along with transporting material. The vibratory displacement is measured by non-contact inductive sensor **9.** The granular material comes to the trough from storage hopper **10**. Input flow can be braked off by closing the movable shutter **11**.

3. MODELING OF EVF DYNAMICS

A high performance model-based control requires a detailed analysis of electromagnetic and mechanical part of the EVF.

3.1 ELECTROMAGNETIC PART

Detailed model of electromagnetic actuator is derived in [2]. It can be written as:

$$L(y)\frac{di}{dt}+\left(\frac{\partial L(y)}{\partial y}\frac{dy}{dt}+R\right)i=u\,, \tag{1}$$

$$f=\frac{1}{2}\frac{\partial L(y)}{\partial y}i^2\,, \tag{2}$$

where R and $L(y)$ denotes coil electrical resistance and inductivity, and y, i and u denotes feeder trough position in relation to feeder base, coil current, and coil voltage respectively. Mechanical force f is produced by the electromagnet. Coil voltage u depends on input u_D of the driver:

can be used to obtain the coil current $i(t)$.

$$u=\begin{cases} V_s, u_D=1\vee i<0 \\ -V_s, u_D=0\wedge i>0\,, \\ 0, u_D=0\wedge i=0 \end{cases} \tag{3}$$

where V_s denotes source voltage. As will be shown later, pulses are always triggered around equilibrium position $y=y_0$, so $L(y)$ could be approximated with $L(y)\approx L(y_0)=L_0$.

Pulses generated by control logic are short (a few ms), so having in the mind that the equivalent time constant R/L_0 of the coil is much greater then pulse duration, and for small velocities $\dot{y}$, second term in (1) could be neglected. To illustrate that, a short (4 ms) u_D pulse is triggered on the experimental feeder from Fig. 1, for empty trough. Results are presented on Fig. 2. It is evident that instead of (1), the following differential equation

$$\frac{di}{dt} = \frac{u}{L_0} \tag{4}$$

can be used to obtain the coil current $i(t)$.

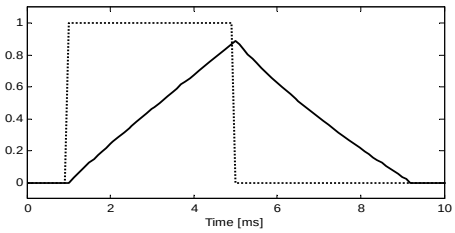

Fig.2. *Experimental trigger response: excitation pulse* u_D *(dotted line) and coil current* i *(solid line)*

3.2 MECHANICAL PART

Detailed dynamic model of the mechanical part of EVF is given in [2], [3]. Essential dynamics can be approximated with only one dominant oscillating mode:

$$\ddot{y} + 2\varsigma\omega_0\dot{y} + \omega_0^2(y - y_0) = K_p\omega_0^2 f \,, \tag{5}$$

where ω_0 (rad/s), ς and K_p denotes resonant frequency, damping factor, and static gain respectively.

However, from the viewpoint of the design and tuning of the control system, we have to analyze the simplified model (5) in the presence of the material in the trough. There are two cases important for our analysis:

- When the amplitude is relatively small, material is moving together with trough (there is no transport). In this case material is acting as additional mass.
- On higher amplitudes, transported material is in fluidized state, reacting with a trough as additional damping force.

To illustrate dynamic characteristics of the process in both cases, trough of our experimental feeder is filled with sugar and feeder is excited with short current pulse as before. Time responses for empty and full trough are compared in Fig. 3. In Fig 3.(b), at the beginning, on higher amplitudes, value of parameter ς is higher (estimated 0.1) and on lower amplitudes ς is lower (estimated 0.01), as for empty trough, Fig. 3.(a).

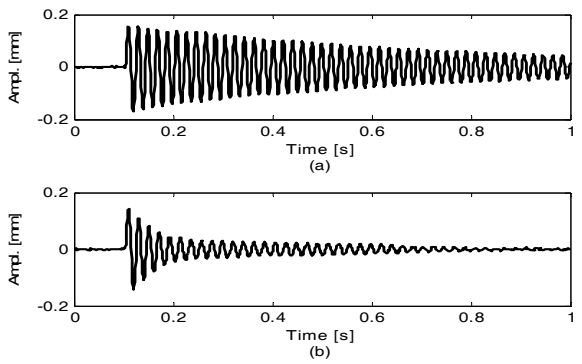

Fig.3. *Experimental Time responses of the EVF: a) empty trough, ς=0.01, b) full of sugar, ς=0.1.*

From the above analysis it follows that the resonant peak, which is inverse proportional to ς, changes for about 10 times. Since the damping ratio is small, further simplification is adopted by setting $\varsigma = 0$ in (5). Finally, as ω_0 is practically independent of the trough content, see Fig. 3.(a) and Fig. 3.(b), model of the mechanical part can be expressed in the following state space form:

$$\dot{x} = \begin{bmatrix} \dot{x}_1 \\ \dot{x}_2 \end{bmatrix} = \omega_0 \begin{bmatrix} 0 & 1 \\ -1 & 0 \end{bmatrix} \times \begin{bmatrix} x_1 \\ x_2 \end{bmatrix} + K_{p1}\omega_0 \begin{bmatrix} 0 \\ 1 \end{bmatrix} i^2 \,, \tag{6}$$

$$y = x_1 + y_0 \,, \tag{7}$$

$$K_{p1} = \frac{K_p}{2} \left. \frac{\partial L(y)}{\partial y} \right|_{y=y_0} . \tag{8}$$

Vibration amplitude a is expressed as function of the state x:

$$a = \sqrt{x_1^2 + x_2^2} \,. \tag{9}$$

Now, it is interesting to analyze the response of the model (6) - (9) excited with Dirac delta pulse on i^2. From (6) and (9), it is obtained

$$a_+ = \sqrt{a_-^2 + 2K_{p1}\omega_0 Q x_{2-} + (K_{p1}\omega_0 Q)^2} \,, \tag{10}$$

where - and + signs in index indicates values immediately before and after pulse, respectively, and Q is pulse strength. From (10) it follows that the highest increase or decrease of the amplitude is obtained when x_2 is in its maximum or in its minimum, respectively. In both cases

$$x_1 = 0 \,, \tag{11}$$

$$x_2 = \pm a_- \,. \tag{12}$$

Thus, from (10) – (12) one obtains

$$a_+ = a_- \pm K_{p1}\omega_0 Q \,, \tag{13}$$

where $\pm$ sign corresponds: + for increasing and – for decreasing the amplitude.

4. CONTROL

General structure of the feeder control is presented on Fig. 4. Structure consists of the state observer OB, triggering part, and PI controller.

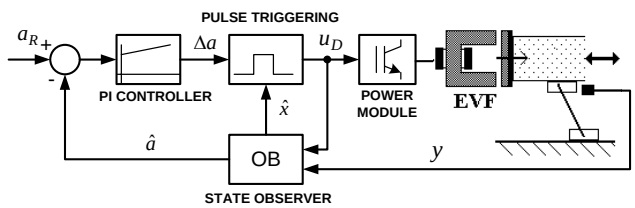

Fig.4. *General structure of feeder*

4.1 OBSERVER

According to (6)-(8), for mechanical part we choose Luenberger observer [4]:

$$\dot{\hat{x}} = \omega_0 \left\{ \begin{bmatrix} -k_1 & 1 \\ -1-k_2 & 0 \end{bmatrix} \hat{x} + K_{p1} \begin{bmatrix} 0 \\ 1 \end{bmatrix} i^2 + \begin{bmatrix} k_1 \\ k_2 \end{bmatrix} (y - y_0) \right\}. \quad (14)$$

Parameters k_1 and k_2 are obtained by defining time constants T_1 and T_2 of the observer as $T_1 = T_2 = \pi/(10\omega_0)$. Thus, it is obtained $k_1 = 6.3694$ and $k_2 = 9.1424$. Coil current i can be measured or estimated using (3) and (4).

Parameter y_0 can also be estimated on line. Its estimation is defined by

$$T_0 \dot{\hat{y}}_0 = y - \hat{y}_0 - x_1, \quad (15)$$

where T_0 is a filter time constant. As y_0 changes relatively slowly, T_0 can be comfortably large. It is suggested here to use

$$T_0 = 10\pi/\omega_0. \quad (16)$$

Finally, the amplitude is estimated by using $a = \sqrt{\hat{x}_1^2 + \hat{x}_2^2}$. As demonstrated experimentally, this enables fast disturbance rejection.

4.2 PULSE TRIGGERING

As will be shown, relationship between pulse duration and amplitude increase/decrease is highly nonlinear. As pulse width T_p in practical applications is very small against cycling period, its contribution can be approximated with Dirac pulse of the same strength. According to (2), (3) and Fig. 3 strength of the pulse can be calculated as follows:

$$Q = 2\int_0^{T_p} i^2 dt = \frac{2}{3}\frac{V_S^2}{L_0^2} T_p^3, \quad (17)$$

or, according to (13) and (17)

$$T_p = \sqrt[3]{\frac{3L_0^2}{2V_S^2 K_{p1}\omega_0}|\Delta a|}, \quad (18)$$

where Δa is desired increment ($\Delta a > 0$), or decrement ($\Delta a < 0$) of amplitude, obtained from the controller, Fig. 4. In this way, (18) defines pulse width – amplitude linearization.

Now, we can define triggering conditions for amplitude increasing:

$$\cos(\omega_0 T_p)\hat{x}_1 + \sin(\omega_0 T_p)\hat{x}_2 \geq 0,\ \hat{x}_1 < 0, \quad (19)$$

or decreasing:

$$\cos(\omega_0 T_p)\hat{x}_1 + \sin(\omega_0 T_p)\hat{x}_2 \leq 0,\ \hat{x}_1 > 0, \quad (20)$$

providing that at center of current pulse (end of u_D pulse after time T_p) (11) is satisfied.

4.3 PI CONTROLLER

Simplest control low is a proportional one:

$$\Delta a = K_C(a_R - \hat{a}), \quad (21)$$

where K_C, a_R, and $\hat{a}$ denotes controller gain, reference amplitude and observed amplitude respectively. The value of Δa and corresponding T_p are calculated in the real time until pulse is started. During the pulse T_p is unchanged. Upper limit for controller gain is $K_C = 1$, meaning that after the pulse, control error have to be zero. In practice, due to the modeling errors and adopted approximations in calculations, recommended gain interval is $K_C \leq 0.8$. To have offset-free control, integral action is introduced, so PI control law is given by

$$\Delta a = K_C\left[(a_R - \hat{a}) + \frac{1}{T_I}\int (a_R - \hat{a})dt\right], \quad (22)$$

where T_I denotes integral time constant of the controller. It is recommended to choose integral constant

$$T_I = 10\pi/\omega_0. \quad (23)$$

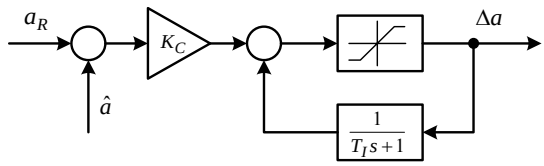

Fig.5. *Anti-windup structure of the PI controller.*

Anti-windup implementation of PI controller presented in Fig. 5. is used as in [5], with saturation element providing limit on controller output and accordingly to (18), with pulse duration T_p.

3. SIMULATION RESULTS

To illustrate the basic operation of the proposed controller, simulations are performed using simplified models of the electrical part (3) – (4) and mechanical part (5), developed in Section IV. In this analysis: $K_p = 1$, $\omega_0 = 314\,\text{rad/s}$, $\varsigma \in [0.01, 0.1]$, $f = i^2$ and $V_S / L_0 = 122$. Controller, derived in Section V is implemented in digital form, with sampling period $T_S = 0.1\text{ms}$ and 0.025mm conversion resolution. Pulse duration (on u_D) is limited on 4ms.

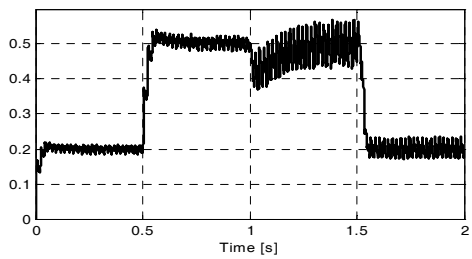

Fig.6. *Simulated amplitude response on reference change and disturbance (change in damping coefficient).*

Fig. 6 illustrates behavior of the control loop in presence of reference changes and disturbance. At $t = 0.5\text{s}$ reference of amplitude is changed from $a_R = 0.2\text{mm}$ to $a_R = 0.5\text{mm}$, and at $t = 1.5\text{s}$ back to $a_R = 0.2\text{mm}$. At $t = 1\text{s}$ there is step change in damping ratio from $\varsigma = 0.01$ to 0.03. Only

estimated amplitude is presented. Integral part of the controller provides that the **mean value** of amplitude coincides with its reference.

Set point response is fast, with small overshoots in both cases (rising and decreasing). Disturbance response has small maximum error and recovery time defined by integral time constant ($T_I = 0.1\text{s}$).

5. EXPERIMENTAL RESULTS

5.1. EXPERIMENTAL SETUP

To demonstrate the performance of the proposed feedback controller, experimental setup presented on Fig. 1. is used. Control algorithm is implemented on industrial PC platform with 12bit A/D interface for displacement measurement and Linux + RTAI operating system software. Displacement is measured with inductive distance sensor.

Parameters K_{p1} and ω_0 in (6) – (8) are estimated from experiment with empty trough. System is excited with $T_p = 4\text{ms}$ pulse on u_D, $V_S = 300\text{V}$, and response is recorded. Parameter $\omega_0 = 320\,\text{rad/s}$ is determined directly from cycle duration. Immediately after the pulse, amplitude Δa reaches its maximum, so K_{p1} is obtained according to (18). Parameter L_0 is estimated from coil current response.

5.2. SET POINT CHANGE

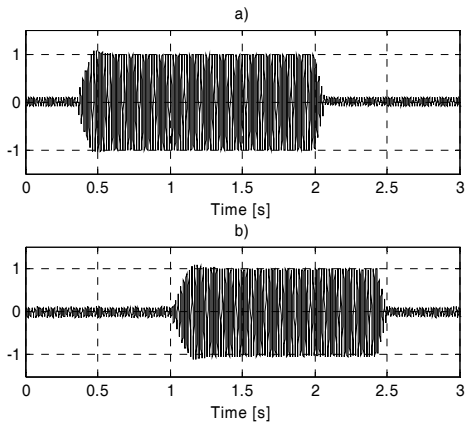

Fig.7. *Simulated Experimental reference change responses for a) empty trough, b) full trough.*

Reference change tests are made for empty and for full trough. Reference is changed in steps from 0.1mm to 1mm and back to 0.1mm. Results are presented on Fig. 7. Both responses are well damped and with a small overshoots.

5.2. DISTURBANCE RESPONSE

A 250g sugar bag dropped onto trough is used to demonstrate disturbance response of the feeder. After about 1 - 1.5s, bag is removed from trough. Results are presented on Fig. 8, only for amplitude reference $a_R = 0.1\text{mm}$ and for empty trough, where the effect of disturbance is the highest. Compared with solution from [2]-[3], results can be judged as excellent

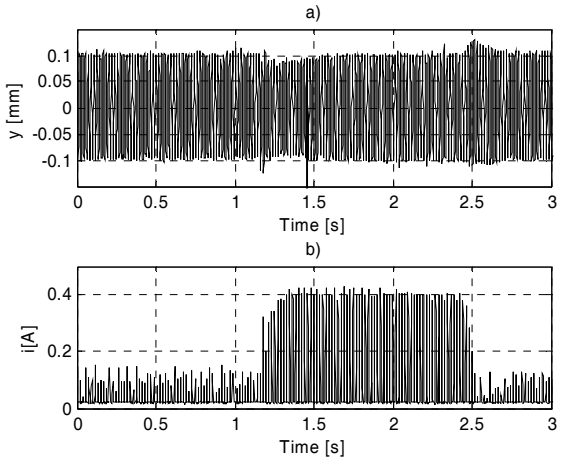

Fig.8. *Disturbance response of empty trough a) displacement, b) coil current.*

6. CONCLUSION

A simple electromagnetic vibratory feeder structure is analyzed in this paper. Despite the low price and low maintenance cost, this kind of feeder is often poorly controlled (frequently without feedback), reducing in that way applicability in precise weighting. A new control structure, based on state observer and PI controller, proposed in this paper, significantly improves feeder performance, enabling high weighting accuracy.

REFERENCES

[1] I.F. Goncharevich, K.V. Frolov, and E.I. Rivin, *Theory of vibratory technology,* Hemisphere Publishing Corporation, New York, 1990.

[2] T. Doi, K. Yoshida, Y. Tamai, K. Kono, K. Naito, and T. Ono, "Modeling and Feedback Control for Vibratory Feeder of Electromagnetic Type", *Journal of Robotics and Mechatronics,* vol. 11, no. 5, pp. 563-572, June 1999.

[3] T. Doi, K. Yoshida, Y. Tamai, K. Kono, K. Naito and T. Ono, "Feedback Control for Electromagnetic Vibration Feeder", *JSME International Journal*, Series C, vol. 44, no. 1, 2001, pp. 44-52.

[4] D. G. Luenberger, "Observing the State of a Linear System," *IEEE Trans. Military Electronics*, vol. 8, pp. 74–80, April 1964.

[5] C.Edwards, I. Postlethwaite, "Anti-windup and Bumpless-transfer Schemes ",*Automatica* , vol. 34, no. 2, pp. 199-210, 1998.

Sadržaj – *Visoke performanse novog regulatora demonstrirane su kroz simulacije i eksperimentalno.*

UPRAVLJANJE ELEKTROMAGNETNIM VIBRACIONIM DODAVAČEM PRIMENOM PI + OPSERVER REGULATORA

Aleksandar I. Ribić, Željko V. Despotović, *Institut Mihajlo Pupin, Beograd.*